DESIGN AND SIMULATION OF FINNED-TUBE HEAT EXCHANGERS USING PURE AND MIXED REFRIGERANTS

A. Bensafi, S. Borg

CETIAT, 27-29 Bd du 11 Novembre 1918, BP 2042, 69603 Villeurbanne Cedex France

ABSTRACT

A computational model for the detailed design of finned-tube heat exchangers is presented. Coils are discretised into tube elements for which the governing equations are solved using local values of temperature, pressure, physical properties and heat transfer coefficients. Single phase, condenser and evaporator cases can be treated using water, R22, R134a, and various refrigerant mixtures based on R32, R125, and R134a. The software can handle non-conventional coil circuits with different numbers of inlets and outlets, non-uniform air distribution at coil inlet face, using smooth and internally finned tubes. All data is supplied through a user-friendly PC-Windows based graphical interface, allowing very flexible design and selection of various circuit configurations. User-defined heat transfer and pressure drop correlations can also used for both the internal fluid and air. This paper also presents new validation results from experiments using water and R22, with and without moisture condensation on the fins. Comparisons with tests show errors of less than 5% on the coil duty. A performance simulation of a coil using R22 and a ternary mixture is presented to validate the programme algorithms developed for mixtures.

INTRODUCTION

Finned tube heat exchangers are most often used in air conditioning and heat pumping. Compared to other system components, these heat exchangers are more complicated to model, due to the complexity of the two-phase flow involved and the heat exchange process between the air stream and the refrigerant, and the flow configuration. On a tube-by-tube basis, strict cross-flow exists locally. However, because of constraints as well as for heat transfer efficiency, manufacturers often adopt various pipe circuiting methods. This diversity further complicates the flow configuration - and classification.

Moreover, and due to new world-wide regulations on the use of chlorine-containing working fluids, there has recently been an increasing interest in new, environmentally benign refrigerants. Proposed alternative substances for R22 include zeotropic refrigerant mixtures (ZRMs), with R407C being proposed as the best candidate for the medium term. In terms of thermodynamic behaviour, there are two basic differences between a pure fluid and ZRMs, which manifest themselves at phase change:

- mixtures undergo phase change with a 'gliding' temperature;
- vapour and liquid compositions are different for a two-phase mixture, and will continuously change throughout the heat transfer process, which influences the properties of the two phases.

These phenomena introduce further complexity to the design of evaporators and condensers using ZRMs.

Current coil design models generally fall into two broad categories: zone-based and detailed models. The zone-based models divide the coil into several parts corresponding to the phases that the refrigerant exhibits throughout the heat transfer process (vapour, liquid, and two-phase). Each zone is then treated as a separate heat exchanger. One such model is CANUT[1], which is based on the NTU (Number of Transfer Units) method. However, and because of their oversimplifying

assumptions and approach, the use of these models is limited to classical configurations and simple coil circuiting. In coils where moisture condensation occurs, their results can sometimes be deceptive.

Detailed models are more rigorous because they divide the whole heat exchanger into tubes or even parts of tubes with their associated fins, where local properties are used. For each tube, or part of tube considered, the thermal and fluid flow performance are computed using local values of temperature, pressure, properties and heat transfer coefficients (HTCs). Ellison et. al[2], Domanski and Didion[3], Huang and Pate[4], Oskarsson et al.[5,6] and Domanski[7] presented various models. None of their programmes could handle mixtures. Haselden et al.[8] presented a detailed simulation programme for both evaporator and condenser design. The model could treat parallel symmetrical configurations with intermediate joining or branching in individual circuits, and could handle refrigerant mixtures. Horizontal and vertical flow orientation could be treated. Air velocity and temperature distribution at the coil inlet face was assumed to be uniform, with the air HTC value being supplied as an input parameter. By performing tests with a R22/R142b binary mixture in circuited vertical coils using louvered fins and internally finned tubes, Haselden et al.[8] derived heat transfer coefficient enhancement factors and subsequently designed novel heat exchangers for air conditioning duties[9]. However, the number of possible design configurations was limited and manual iterations were necessary. Further work was also required to handle properly the effects of condensation of moisture on the fins.

A zone-based model[1] is currently used at CETIAT for coil simulation and design. However, because it heavily relies on experiments and can only treat symmetrical circuits, it was desirable to develop a detailed model to conduct simulations of evaporators and condensers with better accuracy, using either user-supplied or literature correlations. Desirable features of this computational tool are the ability to handle mixtures, non-uniform air temperature and velocity distributions at the coil inlet face and complex circuits. CYRANO is currently being developed to that effect. The programme main features and preliminary validation were shown previously by Bensafi et al.[10]. The present work introduces the methods followed to derive heat transfer correlation parameters from experimental data, and shows results obtained from additional experiments carried out on sixteen coils using water and R22, with smooth and grooved tubes.

COMPUTATIONAL APPROACH

Since design procedures for both evaporator and condenser are very similar, both models have been included into a single programme. Figure 1 shows a view of the coil discretisation into tubes and elements with their associated fins. Starting at the air inlet face, index n represents row number. Index j represents tube number on any considered row, while i is the element number on that tube. Thus each tube element will be identified by this triplet (n,j,i). Figure 2 shows the division of tubes into elements. Considering a coil with Nr rows, Nt tubes per row and Ne elements per tube, the discretisation procedure implies that there will be three-dimensional matrices for air temperatures (dry and dew point) and flow rates requiring dimensions (Nr+1, Nt, Ne) and for refrigerant temperatures, pressures and vapour qualities requiring dimensions (Nr, Nt, Ne+1).

Energy balance and heat transfer rate equations for tube elements

For any element i, one can write two rate equations, a heat balance, and a pressure balance (see Nomenclature for meaning of symbols). For the heat exchanged between the air and the refrigerant :

$$h_a \Delta A_o \left(T_{wi} - T_{ai} \right) = M_a \Delta H_{ai} \qquad (1)$$

$$h_r \Delta A_i \left(T_{ri} - T_{wi} \right) = M_r \Delta H_{ri} \qquad (2)$$

therefore,

$$h_r \Delta A_i \left(T_{ri} - T_{wi}\right) = h_a \Delta A_o \left(T_{wi} - T_{ai}\right) \quad (3)$$

Eliminating the wall temperature from Equations 1 and 2 and using finite differences yields:

$$\Delta Q_i = F_c \Delta T_{LMi} U_i \Delta A_i \quad (4)$$

where U_i is the overall HTC, and $\Delta T_{LMi} = \dfrac{\Delta t_1 - \Delta t_2}{\ln\left(\dfrac{\Delta t_1}{\Delta t_2}\right)}$ (5)

with $\Delta t_1 = T_{r,i+1} - T_{a,in,i}$ (7)

and $\Delta t_2 = T_{r,i} - T_{a,out,i}$ (8)

and where F_C is a correction factor to account for the effect of cross flow (it is essentially unity for a phase-changing refrigerant, but can deviate from unity in the single phase region). The mean temperature difference for heat transfer in element i is ΔT_{LMi}. The above equations assume that h_a, the air HTC includes all the thermal resistances, i.e. the wall, fins, contact and air resistances and takes into account the fin efficiency. When moisture condensation occurs, the heat transfer rate (as expressed by equation 4) will be based on 'enthalpic transfer', following the method outlined by Threlkeld[11].

The heat transfer rate can also be obtained from partial energy balances:

refrigerant: $M_r \Delta H_{ri} = \Delta Q_i$ (9)

air: $M_a \Delta H_{ai} = \Delta Q_i$ (10)

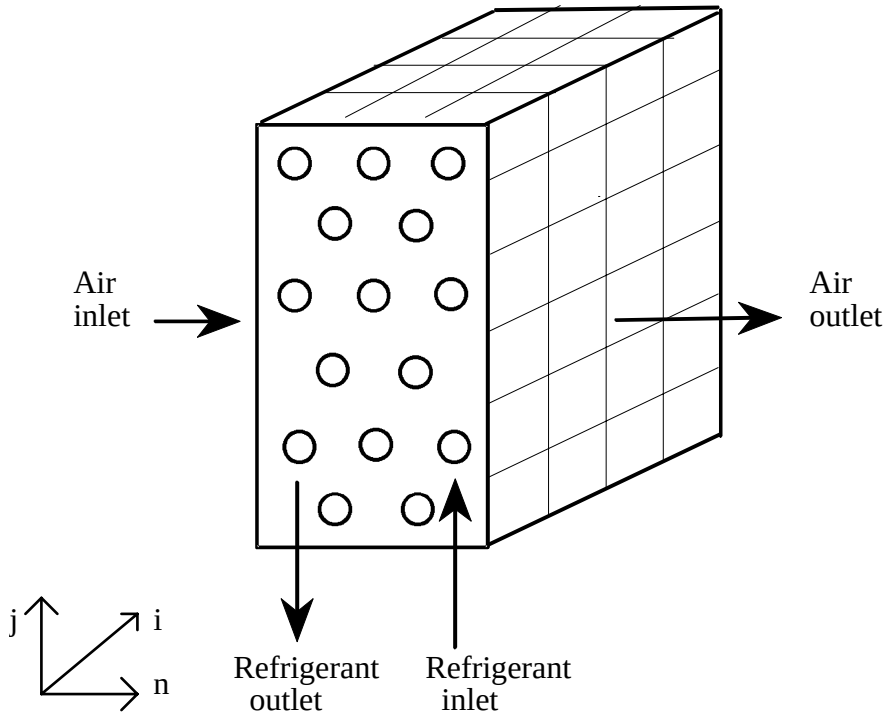

Figure 1: Coil discretisation

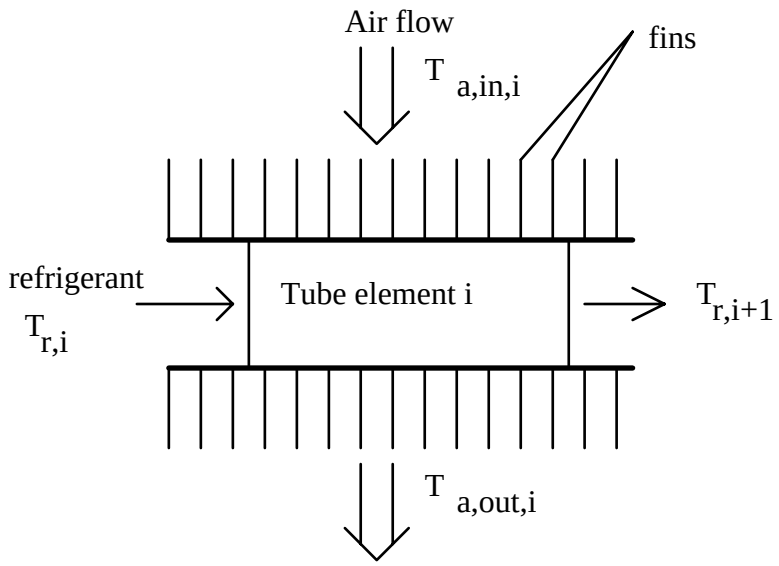

Figure 2: Discretisation of tubes into elements

Data input procedure

CYRANO requires data about the coil geometry and circuitry, and the operating conditions for which simulation is to be carried out. This information is supplied through an user-friendly WINDOWS-based graphical interface. Starting with a conventional circuit, the user is given the opportunity to modify the circuits by eliminating 'bonds' between successive tubes and creating other bonds to form a tailored new circuit configuration, with the possibilities of intermediate tube branching or joining. Required inlet operating data are refrigerant (or water) mass flow rate, temperature, pressure and vapour quality, and air temperature, humidity (expressed as water dew point), velocity and pressure. Refrigerant conditions at each inlet tube and air conditions at the inlet face of tube elements must be specified. It is therefore possible to specify a non-homogeneous air distribution at the coil inlet face (in temperature as well as in velocity).

An additional feature of the programme is the possibility to accommodate user-defined heat transfer and pressure drop correlations for the tube and fin sides. However, this item will not be discussed herein.

Computation algorithm

All the necessary geometrical parameters are first calculated. The three-dimensional matrices of temperature, vapour quality, and pressure are initialised depending on the fluid being used and the detected calculation case (condenser or evaporator). By starting at the inlet tube, the programme tracks the refrigerant until outlet. Depending on the vapour quality, single phase or two-phase routines will be called. The outlet air and refrigerant temperatures and vapour qualities are determined and used to update the matrices. All parallel circuits are treated in this manner from inlet to exit. The calculations scheme is then repeated in a second loop, starting at the air inlet face, and independently of the refrigerant flow direction. These two successive loops continuously update the matrices of temperatures, pressure, vapour quality and air humidity. By comparing successive values of these parameters, residuals are calculated. Convergence is obtained when these residuals reach pre-specified tolerances, which are set to 0.005 K for temperatures and 0.001 for vapour quality.

Upon convergence, the programme yields the total heat duty, the refrigerant outlet temperature, pressure and vapour quality (averaged, if more than one circuit), and the air outlet temperature and humidity. For coils with multiple circuits, the refrigerant flows in the different branches are recalculated to result in individual circuit pressure drops that compare with the average pressure drop value, within a specified tolerance.

HEAT TRANSFER AND PRESSURE DROP CORRELATIONS

Pressure drop

For horizontal flow, and neglecting gravitational effects, the total pressure drop occurring in any element is the sum of acceleration and frictional terms.

The acceleration component accounts for the pressure recovery or loss due to the change in momentum. Its calculation requires the void fraction, which is estimated from Smith's equation as cited by Koyama et. al[12]:

For single phase flow, the friction factor is first determined depending on the magnitude of the Reynolds number. For Re<2300, the Poiseuille correlation is used. For Re>10000 the Blasius correlation is used.

For two-phase flow, the frictional component was calculated as a function of the Lockhart-Martinelli pressure drop parameter X_{tt} given by:

$$X_{tt} = \left(\frac{1-x}{x}\right)^{0.9}\left(\frac{\rho_v}{\rho_l}\right)^{0.5}\left(\frac{\mu_l}{\mu_v}\right)^{0.1} \tag{11}$$

When the vapour mass fraction is below 75%, the pressure drop is calculated from the Martinelli and Nelson correlation as cited by Jung et. al[13] as :

$$\frac{\left(\Delta P_{i,fri}\right)_{tp}}{\left(\Delta P_{i,fri}\right)_{l}} = \left(\Phi_{tp}\right)^2 \tag{12}$$

with

$$\left(\Phi_{tp}\right)^2 = 12.82\, X_{tt}^{-1.47}(1-x)^{1.8} \tag{13}$$

where the subscripts *tp* and *l* refer to two-phase and liquid, respectively.

The two-phase multiplier $(\Phi_{tp})^2$ is calculated at 4 intervals in each element; then, the two-phase frictional pressure drop $(\Delta P_{i,fri})_{tp}$ as recommended by Jung et. al[13] is computed from:

$$\left(\Delta P_{i,fri}\right)_{tp} = \frac{2\,fG^2\Delta L_i}{D\rho_l\Delta x}\int_{x_i}^{x_{i+1}}\left(\Phi_{tp}\right)^2 dx \tag{14}$$

When the vapour quality is greater than 75%, the two-phase frictional pressure drop is calculated from :

$$\frac{\left(\Delta P_{i,fri}\right)_{tp}}{\left(\Delta P_{i,fri}\right)_{vo}} = \left(\Phi_{vo}\right)^2 \tag{15}$$

where the subscript *tp* and *vo* refer to two-phase and vapour only, respectively. The two-phase multiplier was calculated as recommended by Soliman[14]:

$$\left(\Phi_{vo}\right)^2 = 1 + 2.82\, X_{tt}^{0.525} \qquad (16)$$

Once the tube frictional component of the pressure drop is calculated, the corresponding return bend pressure drop is computed with an equivalent $(L/D)_{eq}$ ratio taken as 50, following current engineering practice[15].

Refrigerant heat transfer

Single phase

For Re < 2300 , the Hausen correlation for laminar flow, as cited in Shah and London[16], is used. For the transition case, where 2300 ≤ Re ≤ 10000, the single phase Nusselt number, Nu, is evaluated from the Gnielinski[17] semi-empirical correlation. For the fully developed turbulent flow, i.e., when Re > 10000, the Petukhov correlation[18] is used:, both the Gnielinski and the Petukhov correlations are corrected for the effect of tube length.

Condensation

Following the recommendations of Nitheanandan[19], a set of correlations has been used to account for the effects of the flow regime. Correlations from Akers and Rosson[20], Soliman[21], and Shah[22] are used for wavy, mist and annular flows, respectively.

Evaporation

Jung and Radermacher[23,24] reported numerous experiments with evaporating refrigerants. Their correlation is used from low vapour qualities up to 90%.

Transition region:

As the refrigerant evaporates, its vapour mass fraction increases, and so does the accompanying HTC. However, towards the end of the evaporation process, it reaches a region where the liquid film on the tube walls disappears. This phenomenon is called 'dry-out', and induces a sharp decrease in the HTC. An extensive literature survey was conducted by one of the authors (Bensafi[25]). The results showed very conflicting predictions, with the transition quality ranging from 0.75 to 0.98, depending on the prevailing mass and heat fluxes.

Since the Jung and Radermacher correlation has been validated for qualities ranging from 20 to 90% for a wide range of conditions and refrigerants, a fixed transition quality of 90% was adopted.

Beyond this vapour quality, the HTC is calculated by a linear interpolation between the vapour phase and the transition quality HTCs:

$$h_r = 10\left[(1-x)h_{0.9} + (x-0.9)h_{vap}\right] \qquad (17)$$

Enhancement factors for micro-finned tubes

In order to take into account the effect of enhanced tubes on the refrigerant HTC, constant enhancement factors can be entered as input parameters, or can be calculated. For evaporation and single phase flow, the enhancement factor is calculated from the inside surface area augmentation factor due to the presence of the grooves (from their height, number, apex and helix angles). For condensation, the enhancement factors are calculated as suggested in Cavallini et. al[26]:

$$h_{c,\,finned} = h_{c,smooth} R_x^{\,2} \left(BoFr\right)^{-0.26} \qquad (18)$$

with $Bo = \frac{gl\pi\rho_l d}{8n_g\sigma}$ $Fr = \frac{v_{vo}{}^2}{gd}$ $Rx = \frac{\left\{\frac{\left[2n_g l\left(1-\sin\left(\gamma/2\right)\right)\right]}{\pi d\cos\left(\gamma/2\right)}+1\right\}}{\cos(\beta)}$ (18,19 and 20)

where $h_{c,smooth}$ is the condensation HTC calculated for a smooth tube, l the fin height, d the inside diameter, n_g the number of grooves per tube, γ the helix angle, β the fin angle and σ the refrigerant surface tension. The Froude number Fr is calculated on the basis of the vapour flowing alone. The Rx factor accounts for the heat transfer surface area increase due to the grooves, and the Bond number Bo for the effect of liquid surface tension.

Air side under dry conditions

The convective HTC for the air side may be calculated in terms of the "j-factor" as follows:

$$h_{air,dry} = \frac{jG_{a,max}C_p}{Pr^{2/3}} \tag{21}$$

where $G_{a,max}$ is the air mass flux calculated at the minimum flow area. The j-factor depends on the coil under consideration and, despite attempts by many researchers, it is still difficult to find a universal form that yields consistent and accurate results. This is due to the diversity of fins (flat, wavy, louvered, etc.), the manufacturing techniques, and the large combination of coil geometries.

Air side HTCs can be calculated using the following j-factor form:

$$j = a\,Re^n \tag{22}$$

where a and n are user-defined. Such coefficients can be found in the literature for common fin configurations, or can be derived from experimental results. See later the discussion on the identification of correlation parameters.

Overall HTC for dry conditions

Neglecting fouling and fin-contact resistances, the overall HTC based on the total outside heat transfer surface is then:

$$U = \left(\frac{1}{h_r A_{\text{int}}/A_o} + \frac{1}{\eta_s h_a} + \frac{e_{tube}}{k_{tube}A_m/A_0}\right)^{-1} \tag{23}$$

where the surface effectiveness is expressed as:

$$\eta_s = \frac{A_{b,t}/A_{fins} + \eta}{A_{b,t}/A_{fins} + 1} \tag{24}$$

where A_{int} is tube internal area, A_{fins} the fins surface area, A_o the total heat transfer area, $A_{b,t}$ the bare tube area, A_m the mean tube surface area (logarithmic average of tube inside and outside surface areas) and η the fin efficiency. k_{tube} and e_{tube} represent tube thermal conductivity and thickness, respectively. Fin efficiency is calculated by approximating the rectangular fin area associated with a tube element to an equivalent circular area, as suggested by Rich[27].

Air side HTC for wet surfaces

When the average fin surface temperature is calculated to be less than the water dew point of the air stream at the outlet of any tube element, moisture condensation will occur. Under these conditions, the air HTC can no longer be calculated as outlined previously, and a water mass balance must be carried out.

A review of the literature revealed that the enthalpic method, proposed by Threlkeld[11] was most adequate for application with the detailed model. In this procedure, the driving force for heat transfer is assumed to be the difference between the saturated enthalpy of the air flowing over the fins and a fictitious saturated air enthalpy evaluated at the refrigerant temperature. Consequently, HTCs are transformed to be based on 'enthalpic transfer' in order to take into account the transfer of mass from the air stream to the fins when condensation occurs.

REFRIGERANT MIXTURES

Thermodynamic behaviour

When a refrigerant mixture undergoes phase change, its temperature varies and the composition of the liquid and vapour phases are different. Figure 3 shows a temperature-concentration diagram for a binary mixture of components A and B. Consider a mixture at the inlet of an evaporator, say at point E on figure 3. As it evaporates, the vapour quality increases and the mixture reaches point C. There, the saturated vapour and liquid phases will be represented by points V and L, respectively, and the corresponding compositions of component B will be y and x, respectively. As the mixture is further vaporised, it reaches its dew point at P, where only a vapour phase exists. If it is further superheated, it will reach state M, totally in the vapour phase. As this diagram shows, the mixture composition in the two phases continuously changes from inlet to outlet -and so do the corresponding thermodynamic and transport properties. For mixtures with a small difference between dew point and bubble point, the so-called 'temperature glide', the composition difference between vapour and liquid will not be so important. But with larger glides, they must be taken into account.

The heat transfer process to mixtures therefore introduces more complexity to the computation procedure. The detailed design model which was introduced previously must be modified to account for the different thermodynamic refrigerant behaviour. It is beyond the scope of this work to show in detail all the required modifications to be brought to the procedures shown previously, hence only some of them will be explained.

Adaptation of the detailed design model to ZRMs

The main changes to the calculation procedure involve the following:

- refrigerant property calculations
- initialisation of the refrigerant and air temperature profiles
- calculation of temperature and vapour quality at the exit of each tube element in the two-phase region
- condensing and evaporating refrigerant HTCs

Refrigerant property calculations

A specific programme[28] was written to calculate thermodynamic and transport properties of ternary and binary mixtures based on R32, R125 and R134a. It is based on a cubic equation of state and uses refrigerant manufacturers data for the transport properties. It was then integrated to CYRANO.

Initialisation of temperature profiles

Depending on whether it is condensing or evaporating, the refrigerant reference temperature for initialisation will be equal to the dew point temperature at input pressure (condenser), or to the entering temperature (evaporator). This reference temperature is used as a basis to initialise the refrigerant and air temperatures.

Temperature and vapour quality at exit of tube elements in the two-phase region

This procedure is probably the most complex to adapt to mixtures. Each heat exchanger element is treated as a non-adiabatic separator, as shown in figure 4.

First, an equilibrium calculation is made to determine the liquid and vapour phase composition. These compositions will in turn be used to calculate transport properties for each phase. Pressure drops are then calculated, using the correlations for pure components and the mixture properties. Refrigerant and air HTCs yield heat transfer rates, which are used in partial air and refrigerant energy balances to calculate enthalpies at exit of tube elements.

For ZRMs, the exit temperature is no longer the 'saturation temperature' at the exit pressure as was the case for pure components, but is uniquely given by the computed exit enthalpy and pressure, through an equilibrium calculation, which also yields exit vapour quality.

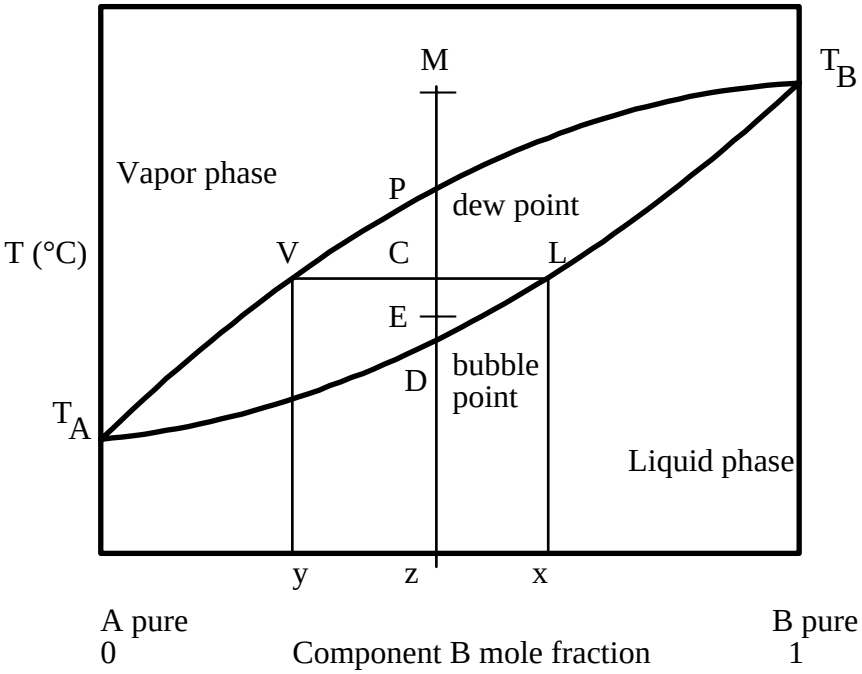

Figure 3 Temperature-concentration diagram for a binary mixture

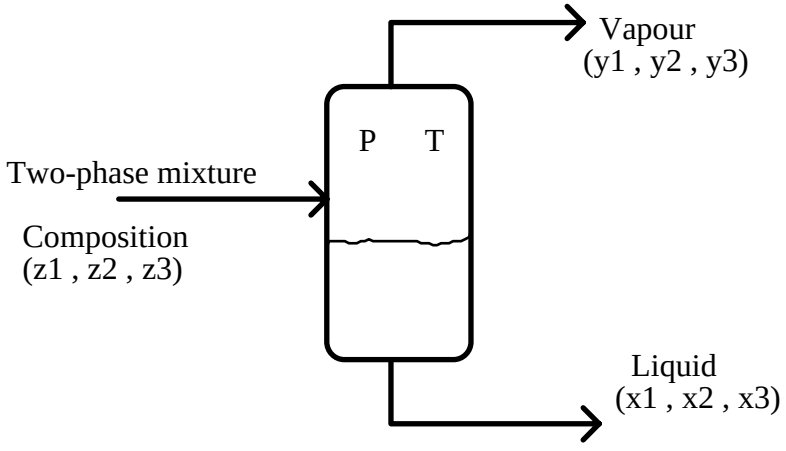

Figure 4: Representation of a tube element as a non-adiabatic separator

Condensing and evaporating HTCs

Numerous reports on condensation and evaporation have shown marked differences between pure fluids and ZRMs, which depend on the nature of the fluids, as well as on operating conditions, such as mass and heat fluxes. Lower HTCs are generally obtained with mixtures, due to the effects of mass transfer resistance, and sometimes to differing mixture properties.

Local condensing coefficients for ZRMs are first calculated from pure component correlations based on mixture transport properties. Then, and following the recommendations of Gayet et al.[29] and Cavallini et al.[26], the local HTCs for ZRMs are calculated using the method developed by Bell and Ghaly[30] to account for the effects of mass transfer resistance. The condensing heat transfer coefficient h_m for the mixture is expressed as:

$$\frac{1}{h_m} = \frac{1}{h_c} + \frac{\Delta T C p_{vap}}{\Delta Q h_{vap}} \qquad (25)$$

where h_c is the condensing HTC for the mixture calculated for a pure component considering the properties of the mixture, h_{vap} is the vapour phase HTC with the vapour flowing alone, ΔT is the temperature difference between inlet and outlet of the tube element, Cp_{vap} the vapour heat capacity and ΔQ is the heat transferred in the tube element.

A similar method is adopted for evaporating coefficients, where a correlation for pure components is first used with mixture transport properties. A corrected HTC is then calculated following the method outlined by Bivens and Yokozeki[31].

IDENTIFICATION OF CORRELATION PARAMETERS FROM EXPERIMENTS

For new fin designs, it is often desirable to be able to predict performance for a whole range of coils based on the same fin. This can be achieved with a small number of experiments using a sample coil with water circulating inside the tubes. Using large water flow rates to minimise the heat transfer resistance on the tube side, the heat transfer resistance and hence the heat transfer coefficient on the air side can be determined. Starting with a base correlation, such as Eq. 22, proper coefficients can then be identified. For many coils, these coefficients have been derived from experiments with water and air. Simulations using these identified coefficients will yield very accurate results.

For the tube side, new designs such as grooved tubes or otherwise enhanced surfaces can also be evaluated using the technique outlined above. For this case, air velocities which minimise the air side heat transfer resistance will be used.

A procedure for identifying correlation coefficients from coil test results is also included in CYRANO. Tube side and air side correlations can therefore be derived. These can in turn be used to predict coil performance for any specified conditions. For manufacturers, this means whole performance catalogues can be generated at the expense of a small number of preliminary experiments. The identification procedure used in CYRANO is distinctive because it cannot rely on classical computation methods to calculate the correlation coefficients. When experiments are carried out, only overall results are known (duty, temperatures at inlet and outlet, flow rates, etc.). During simulation, coils are discretised into a large number of elementary heat exchangers (tube elements), for which the 'local' rates of heat exchange and temperature gradients cannot be determined experimentally. Hence, it is impossible during the identification to use this information and apply a classical method based on least squares. Instead, a multi-parameter minimisation technique is used. For example, and to identify coefficients *a* and *n* used in Eq. 22 for the air side heat transfer coefficient, an objective function Φ would be built as follows:

$$\Phi(a,n) = \sum_{i=1}^{i=N\,\exp} \left(\frac{Q_{calc} - Q_{\exp}}{Q_{calc}} \right)_i^2 \qquad (26)$$

where Q is the heat duty and indexes *exp* and *calc* correspond to experimental and calculated value, respectively. N_{exp} is the number of runs. Coefficients *a* and *n* that minimise function Φ will then be calculated. It is noteworthy that the correlation to be used can utilise more than two coefficients.

For the fluid circulating inside the tubes, a correlation similar to that described by Eq.22 can be used. Whether the fluid is in single phase flow, evaporating or condensing, one can use an equation of the following form to identify proper correlation correcting coefficients:

$$Nu_{ref} = \frac{a_{ref}\,\mathrm{Re}_{liq,tot}^{n_{ref}}\,Nu_{theory}}{0.0243\,\mathrm{Re}_{liq,tot}^{0.8}} \qquad (27)$$

where Nu_{ref} is the Nusselt number for the internal fluid, Re is the Reynolds number; a_{ref} and n_{ref} would be the correlation coefficients (taken by default as 0.0243 and 0.8, respectively). Index *liq,tot* refers to the whole fluid circulating as liquid. Nu_{theory} is the fluid Nusselt number predicted by any one of the correlations listed in the previous sections: Gnielinski[17] for single phase in the transition region, Petukhov[18] for fully developed single phase turbulent flow, Akers and Rosson[20], Soliman[21], and Shah[22] used for condensation with wavy, mist and annular flows, respectively and Jung and Radermacher[23,24] for fluid evaporation. By using only two correcting parameters, this technique allows the use of various correlations. It must be noted, however, that the use of yet other different forms of equations is still possible with the proposed programme.

PROGRAMME VALIDATION

The model preliminary verification consisted in comparing the simulation results with test data from the CETIAT Laboratory for several coils. Experiments were performed under severely controlled conditions in a psychometric room. Duties were calculated from energy balances on both the refrigerant and the air streams, and balances checked within ± 2%. Results are given in reference 11. Additional tests were subsequently performed to validate the identification procedures and are dealt with hereafter.

Determination of air side heat transfer correlation coefficients

A first series of coils was tested using water at high mass flow rates to determine coefficients a and n to be used in the j-factor correlation (Eq. 22). The same fin type was used for all four coils. Tables 1 and 2 shows the characteristics of the three-row coils used in the experiments. Air velocities ranged from 1 to 4 m/s, corresponding approximately to Reynolds numbers between 1000 and 4000, based on the tube external diameter. Coefficients a and n required for the j-factor correlation were then determined for the four coils following the procedure outlined above. These coefficients are shown in Table 1. It must be noted that for Coils 1EAU, 2EAU and 3EAU, tests were carried out with and without moisture condensation on the fins. However, parameter identification was carried out only with results from dry conditions. Simulation was then carried out for both dry and wet conditions.

Figure 5 shows plots of the j-factor vs. Reynolds number for the four coils. As it can be observed, these plots are very similar and begin to deviate slightly only in the very low and very high velocity regions. For air velocities between 1 and 4 m/s, values of the coefficients derived from one coil may perfectly be used for all coils. This was done using coefficients a and n derived from coil 3EAU to simulate all coils at their test conditions (including tests where condensation of moisture occurred). Figure 6 shows the comparison of the measured and calculated duties using CYRANO. For water, one can conclude that the programme can predict performance well within the experimental error

region (2 to 3 %) under dry conditions and with an uncertainty not greater than 5% when moisture condenses on the fins.

***Table 1** : Characteristics of coils tested with water*

Coil	Rows	Tubes	Length	Circuits	Configuration	Coef. 'a'	Coef. 'n'
1EAU	3	12	400	6	counter-flow	2.389	0.681
2EAU	3	12	400	3	cross-flow	2.342	0.681
3EAU	3	12	400	2	counter-flow	2.417	0.681
4EAU	3	18	660	3	counter-flow	1.282	0.596

***Table 2** : Common coil characteristics (3/8" tube)*

tube material		Copper
tube layout		Staggered
Tube inside diameter	mm	9.4
tube thickness	mm	0.35
fin material		Aluminium
fin type	mm	louvered
fin thickness	mm	0.11
fin pitch	mm	1.81
row pitch	mm	22
tube pitch	mm	25.4

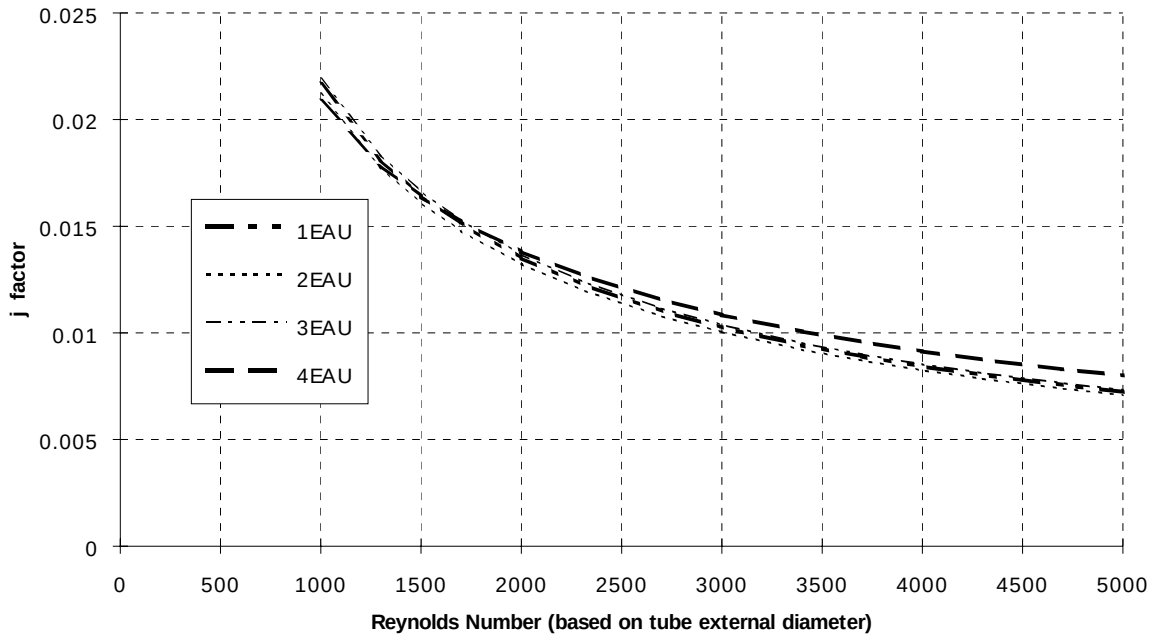

Figure 5: j-factors for the four coils tested with water

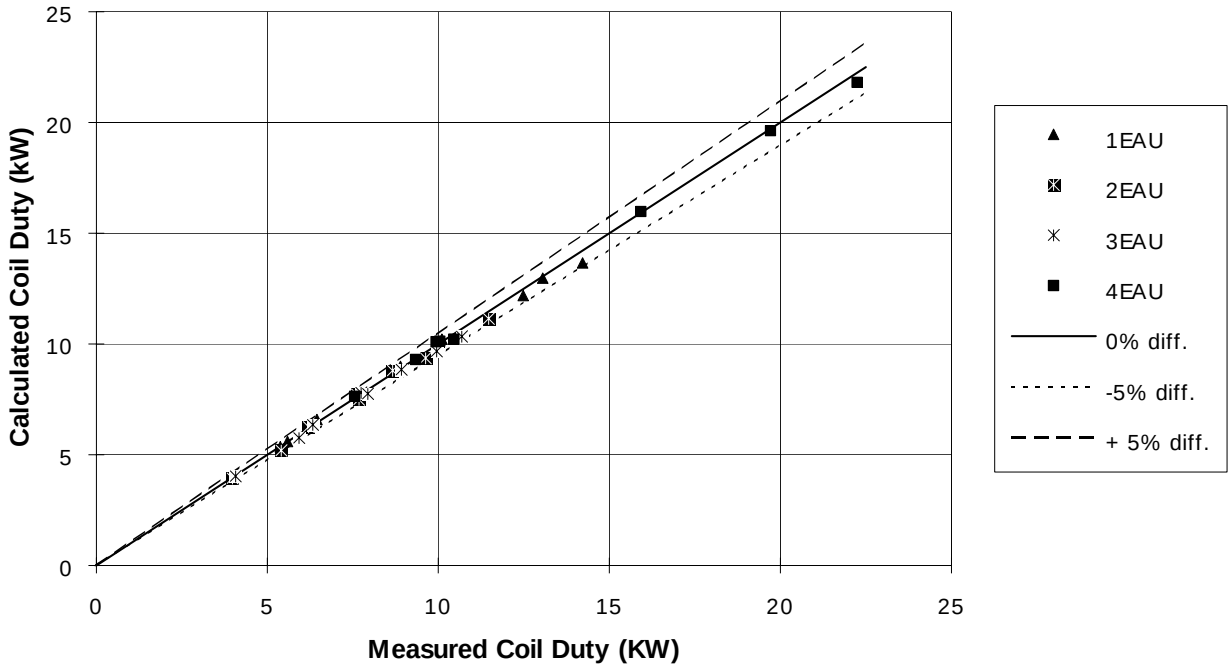

Figure 6: Comparison of measured and calculated duties
for the four coils using coefficients derived from Coil 3EAU

Test results with evaporators and programme validation

A second series of coils was tested using evaporating R22. The coils common characteristics are given in Table 2. Additional information is given in Table 3. All six coils comprise three rows of 12 tubes, with a tube length of 400 mm, with a counter-flow configuration.

***Table 3** : Characteristics of tested evaporator coils*

Coil	Circuits	Tubes	G*
EVAP9	6	smooth	65-140
EVAP15P	6	grooved (18°)++	65-140
EVAP16P	6	grooved (30°)	65-140
EVAP10	2	smooth	210-350
EVAP15	2	grooved (18°)	210-350
EVAP16	2	grooved (30°)	210-350

***** refrigerant mass flux ($kg.s^{-1}.m^{-2}$) ++ groove helix angle

A series of 4 to 8 runs was carried out for each coil, with or without moisture condensation on the fins. The measured duties were then compared to the simulation results using CYRANO and smooth tube correlation for R22. Parameters a and n used for the j-factor expression were taken equal to those of water coil 3EAU. Figure 7 shows that the smooth tube coil performance is well predicted, at both small and large refrigerant mass fluxes, and under wet and dry conditions. Discrepancies for operation under wet conditions are lower than 5% and operation under dry conditions shows better agreement.

For grooved tubes, the simulation using smooth tube correlations yields appreciable errors. The predicted duties are much lower than the measured ones, due to the fact that the grooved tubes appreciably enhance refrigerant heat transfer. Generally, the enhancement brought by the grooving increases the coil duty by about 10%, at the prevailing operating conditions (air velocity slightly above 2 m/s for all runs).

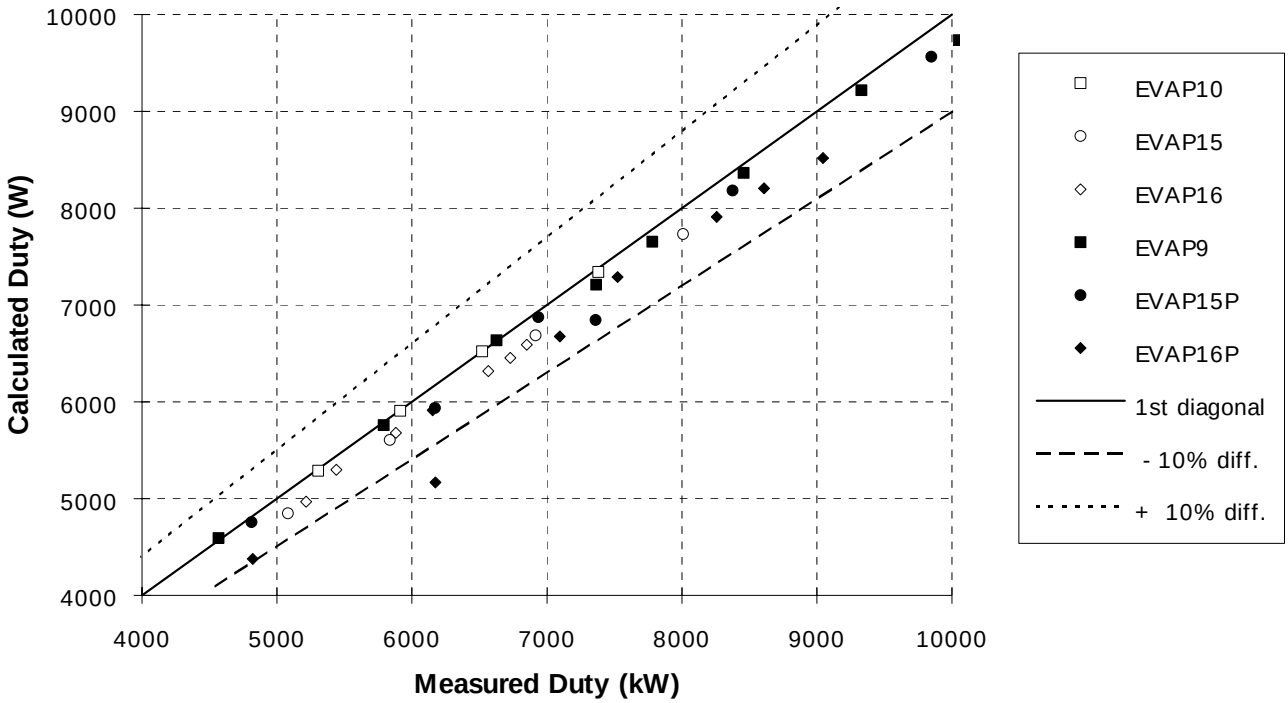

Figure 7: Comparison of measured and calculated duties
for the six evaporator coils using coefficients derived from Coil 3EAU

For evaporation inside grooved tubes, the heat transfer enhancement factor was first set equal to the surface augmentation caused by the presence of the grooves. The results are shown in Figure 8. All calculated duties fall within 0 to +5%. However, a difference between the two types of grooving can now be distinguished. Discrepancies are smaller for the 18° grooving (white symbols) compared to the 30° grooving (black symbols).

An alternative way to correlate data is to identify coefficients, as suggested earlier, and following Equation 27. Coefficients a_{ref} and n_{ref} were calculated only from two test results for each coil, corresponding to the largest and smallest duties in order to cover the full range of mass fluxes. Duties were then calculated with CYRANO. The results are shown in Figure 9. As it can be observed, much smaller discrepancies are obtained compared to those resulting from the surface augmentation factor method mentioned above. Coefficient n_{ref} was found practically equal to 0.8, while coefficient a_{ref} varied from 0.03 to 0.043 (the default value for smooth tubes is 0.0243). The lower enhancement figure is obtained with coil EVAP15P, which corresponds to the lower refrigerant mass fluxes and the 18° helix angle. The largest enhancement figure is obtained with coil EVAP16, which corresponds to the largest refrigerant mass fluxes and the 30° helix angle. It can also be observed that the enhancement brought by the 30° groove helix angle is roughly independent of refrigerant mass flux.

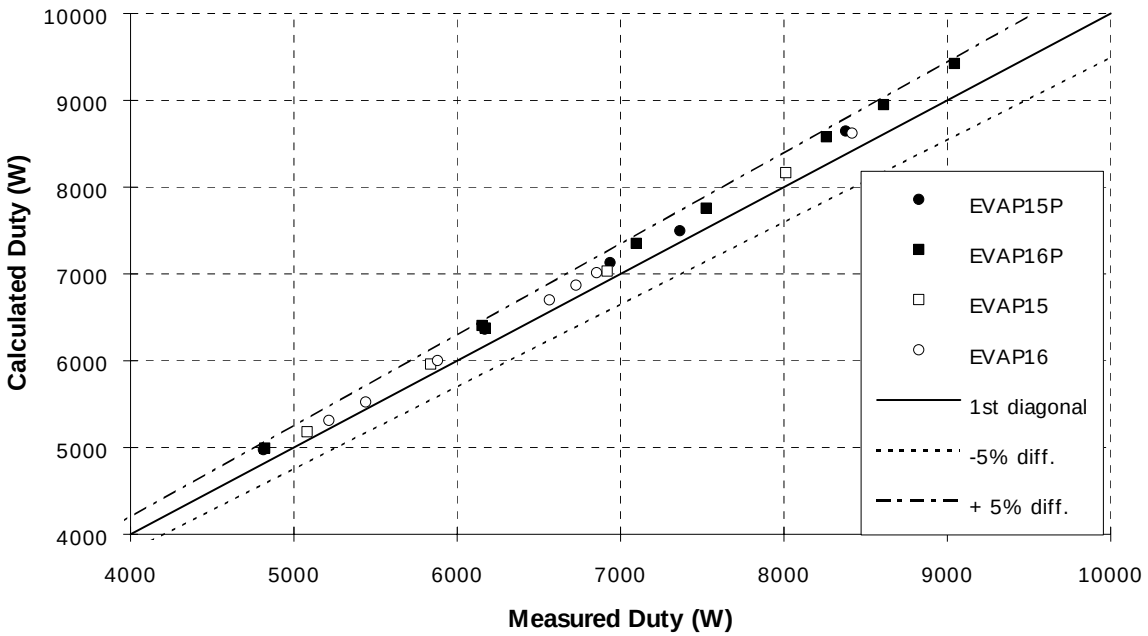

Figure 8: Simulation results using surface augmentation factors for grooved tubes

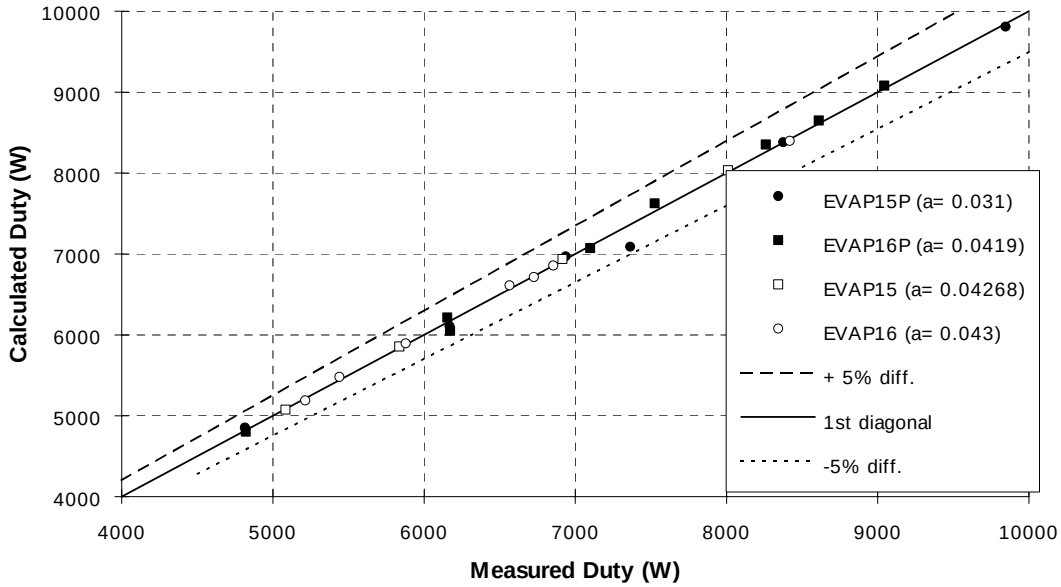

Figure 9: Simulation results using identified coefficients for grooved tubes
(calculated values of a_{ref} for each coil are shown in the legend)

Test results with condensers and programme validation

A third series of coils was tested using condensing R22. The coils common characteristics are given in Table 2. Additional information is given in Table 5. All six coils comprise three rows of 18 tubes, with a tube length of 660 mm and a counter-flow configuration.

***Table 4** : Characteristics of tested condenser coils*

Coil	Circuits	Tubes	G*	Correlation method*
COND9	6	smooth	65-140	a_{ref}=0.0213 and n_{ref} =0.83
COND15P	6	grooved (18°)++	65-140	Cavallini et. al[26]
COND16P	6	grooved (30°)	65-140	Cavallini et. al[26]
COND10	3	smooth	135-270	a_{ref} = 0.023 and n_{ref} =0.83
COND15	3	grooved (18°)	135-270	Cavallini et. al[26]
COND16	3	grooved (30°)	135-270	Cavallini et. al[26]

***** refrigerant mass flux ($kg.s^{-1}.m^{-2}$) ++ groove helix angle ***** for condensation inside tubes

A series of 4 to 8 runs was carried out for each coil. The measured duties were then compared to the simulation results using CYRANO and smooth tube correlations for R22. The air side heat transfer coefficients were predicted using the results derived from tests using water (coil 3EAU). Figure 10 shows that the results from coils using smooth tubes (COND10 and COND9) are well correlated, with discrepancies around 5%.

The results for smooth tube tend to deviate at larger refrigerant mass fluxes (COND10); the predicted duty is consistently 5% below the measured one, which shows that the set of correlations under predicts the refrigerant heat transfer coefficient for large mass fluxes.

Figure 10 also illustrates the enhancement brought by the grooving, which is more important in the case of the condenser coils than for the evaporators, and overall coil duties are underpredicted by as much as 25%. Figure 10 also shows that the heat transfer enhancement factor is more important at low mass fluxes (plain black symbols lay farther than the first diagonal) than at higher ones (hollow white symbols).

The correlation from Cavallini et. al[26] was then tested on the four grooved-tube coils. The base refrigerant condensing coefficient was derived from the correlations cited previously (Akers and Rosson[20], Soliman[21], and Shah[22]) and the correction from Cavallini et al. was applied. For smooth tube coils, an identification was carried out to determine the values of a_{ref} and n_{ref} that best fitted two measured duties among the results from the coils. These values are shown in Table 4. The comparison of calculated and measured duties is shown in Figure 11. As it can be observed, all smooth tube coils results are well correlated using the identified coefficients. The Cavallini et. al[26] correlation for coils with grooved tubes is also very satisfactory for design purposes, yielding discrepancies no greater than 5%.

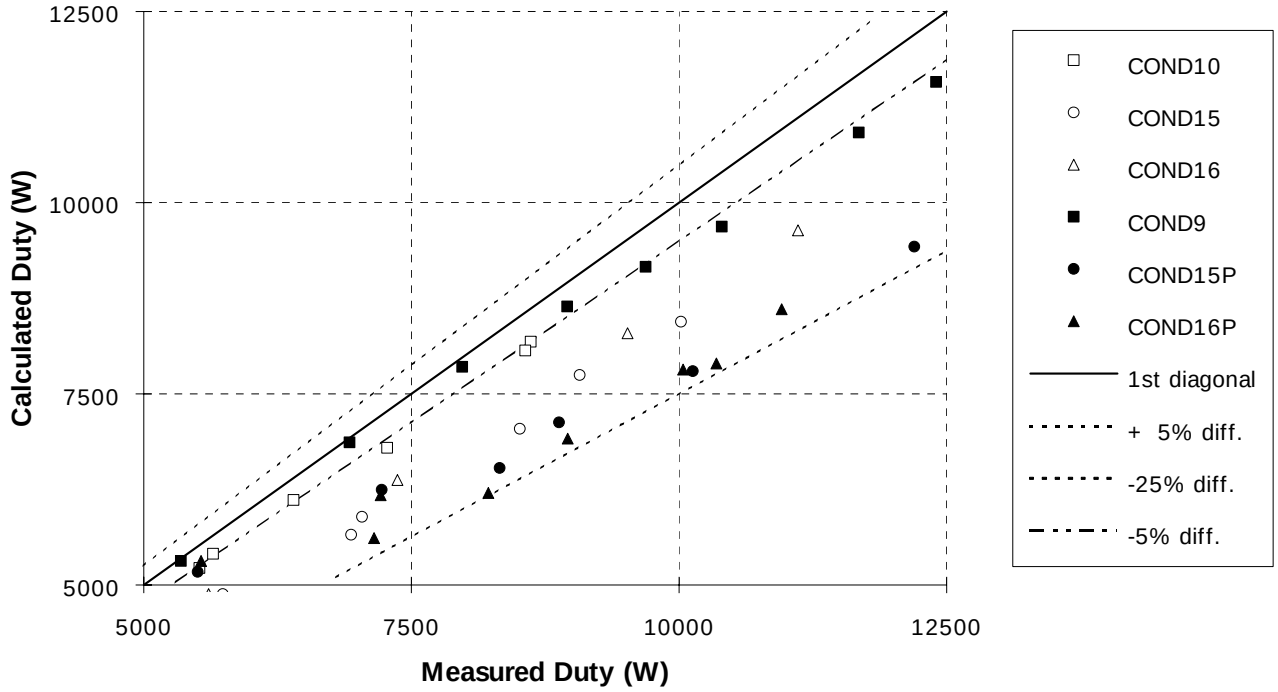

Figure 10: Condenser simulation results using smooth tube correlations

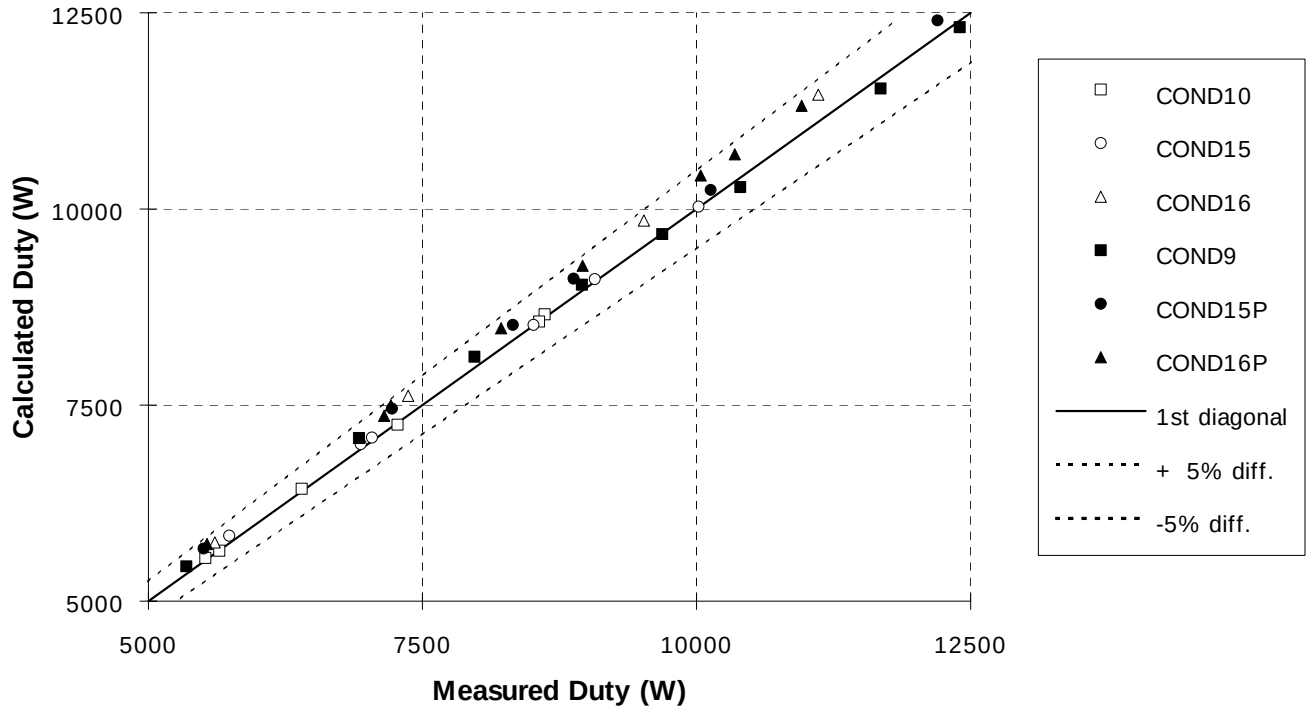

Figure 11: Condenser simulation results using the Cavallini et al. correlation for grooved tubes and parameter identification for smooth tubes

Programme validation for coils using ZRMs

It has not been possible to find experimental work with detailed data on coils using ZRMs. In order to check the developed algorithms, a few simulation cases were run on a coil whose air transfer characteristics were predetermined with water and simulation with evaporating R22 checked against experiments. All cases were based on R22 and R407C. Table 5 shows the inlet operating conditions used for the simulations.

The comparison results are shown in Figure 12. Larger duties are obtained for R407C, under the inlet conditions assumed to illustrate the calculations. In practice, the results may be different because of other interacting cycle components (compressor, expansion valve, etc.). Nevertheless, it noteworthy to mention that the results are very similar to those obtained by Ebisu and Torikoshi[32], who performed experiments with both fluids.

Table 5 : Characteristics of the coil used for simulation

Characteristic of Coil	
Tube length mm	600
Number of rows	2
Tubes per row	15
Configuration	cross-flow
Tubes	smooth
Fins	louvered
Tranverse pitch mm	25
Longitudinal pitch mm	21.6
Tube internal diameter mm	9.38
Tube thickness mm	0.35
Fin thickness mm	0.11
Fin pitch mm	1.80
a/n air parameters (for j-factor)	0.817/0.506

Table 6: Inlet conditions for coil performance simulation using R22 and R407C

Case	Condensation	Evaporation
Air inlet temperature °C	30	20
Air inlet water dew point temperature	5.	5.
Air velocity m/sec	2.5	1.9
Refrigerant flow rate kg/hr	60 to 100	60 to 100
Superheat at condenser inlet °C	35.	-
Temperature at saturation °C	50 ☼	5 ☼☼
Inlet vapour quality	-	0.2

☼ average value of bubble and dew point temperatures at inlet pressure for R407C

☼☼ average value of inlet and dew point temperatures at fluid pressure for R407C

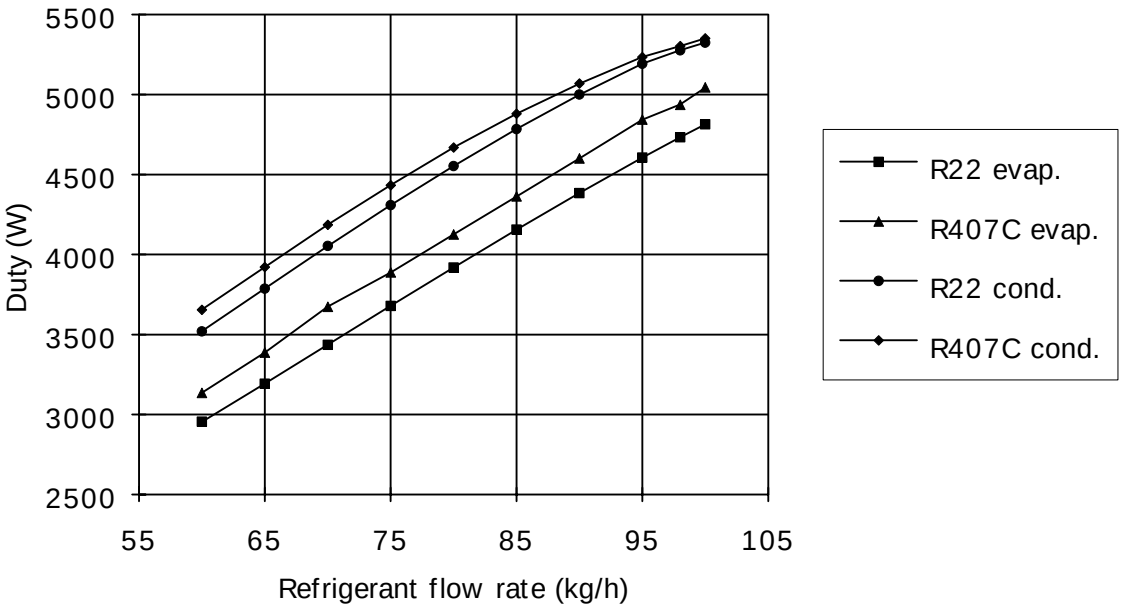

Figure 12 : Performance simulation using R22 and R407C

CONCLUSIONS

A detailed model for the design of plate-fin-and-tube heat exchangers has been developed. The computational approach discretises the heat exchanger into tube elements. Local values of properties and heat transfer coefficients are used. Three-dimensional matrices of refrigerant and air temperatures and pressures are generated. The model makes use of a double-loop iterative scheme which reduces computational time. The model can be used to select among alternative coil circuits at the design stage.

Experiments with coils were carried out with water in order to characterise fins. The identification procedure used by the programme has been presented and validated with results from these runs. Additional experiments were carried out with R22 in both condensation and evaporation inside smooth and grooved tubes. With smooth tubes, the correlations used result in overall duty prediction errors of less than 5%, with or without moisture condensation on the fins. Even better results can be obtained if heat transfer correlation coefficients can be predetermined with a few tests.

For evaporation inside grooved tubes, the refrigerant heat transfer enhancement factor can be taken as the surface augmentation ratio, in the absence of more accurate data. Overall coil duty is predicted within 5% for all cases. With a few tests, proper correlations coefficients can be derived, which generates smaller discrepancies in duty calculations.

For condensation inside grooved tubes, the Cavallini correlation proved to be accurate for two types of grooves, and duties are very well predicted, with calculation errors within the experimental uncertainties. The tests results show that the refrigerant heat transfer coefficient is more enhanced at low mass fluxes than at larger ones. For both the 18 and the 30° helix angles and for the type of grooves tested, heat transfer enhancement is better for condensation than for evaporation.

These experimental results and their validation have shown that the proposed programme can be used with confidence to build performance catalogues for wholes ranges of coils, provided a few test results are available. When used to compare tube inside surfaces, CYRANO proved to be a very fine and useful tool for analysis.

The programme algorithm for the use of mixtures was checked and yielded consistent results. Unfortunately, there were no detailed experimental data with ZRMs to check the programme results. A validation of the programme will be carried out as tests are currently being undertaken.

ACKNOWLEDGEMENTS

This project is being currently undertaken with the assistance of EDF (Electricité de France) and ADEME (Agence de l'Environnement et la Maitrise de l'Energie) and their financial support is gratefully acknowledged.

REFERENCES

1. Armand, J.L., and Molle, N., *Caractérisation des batteries à ailettes à l'aide du logiciel CANUT: applications à la simulation des performances*, Revue Générale de Thermique, N°353, Mai 1991
2. Ellison, R.D., Creswick, F.A., Fisher, S.K. and Jackson, W.L., *A computer model for air-cooled refrigerant condensers with specified refrigerant circuiting*, ASHRAE Trans., 87, pp. 1106-1124, 1981
3. Domanski, P. and Didion, D., *Mathematical model of an air-to-air heat pump equipped with a capillary tube*, Int. J. of Refrigeration, Vol. 7, N°4, pp.249-255, 1989
4. Huang, K. and Pate, M.B., *A model of an air-conditioning condenser and evaporator with emphasis on in-tube enhancement*, Proceedings of IIR Meeting, Purdue, pp. 269-279, 1988
5. Oskarsson, S.P, Krakow, K.I and Lin, S., *Evaporator models for operation with dry, wet and frosted surfaces. Part I: Heat transfer and fluid flow theory*, ASHRAE Trans., 96, Part 1., pp. 373-380, 1990a
6. Oskarsson, S.P, Krakow, K.I and Lin, S., *Evaporator models for operation with dry, wet and frosted surfaces. Part II: Evaporator models and verification*, ASHRAE Trans., 96, Part 1., pp. 381-392, 1990b
7. Domanski, P.A., *Simulation of an evaporator with non-uniform one-dimensional air distribution*, ASHRAE Trans., 97, Part 1, pp. 793-802, 1991
8. Haselden, G.G., Bensafi, A., Foumeny, E.A., *The design of efficient heat exchangers for mixed refrigerants cycles*, Proc. I.Chem.Eng. Conference, Leeds, in Heat Exchange Engineering: Advances in Design and Operation, Vol. 4, pp 1-25, Editors: Foumeny and Heggs, July 1993
9. Bensafi, A. and Haselden G.G., *Further progress with mixed refrigerants for power saving*, Proceedings of the Institute of Refrigeration, Session 1995-96, pp 5-1 to 5-11. London, U.K., February 1996
10. Bensafi, A., Borg, S., Parent, D., *CYRANO: a computational model for the detailed design of plate-fin-and-tube heat exchangers using pure and mixed refrigerants*, accepted for publication in the International Journal of Refrigeration
11. Threlkeld, J.L., *Thermal Environmental Engineering*, 2nd Ed., Prentice-Hall, Inc., 1970.
12. Koyama, S. et al., *Enhancement of in-tube condensation of non-azeotropic refrigerant mixtures with a micro-fin tube*, in Proc.18th Int. Congr. Refrigeration, New Challenges in Refrigeration, Montreal, Vol. 2, pp. 439-443, 10-17 Aug. 1991
13. Jung, D.S. et al., *Prediction of pressure drop during horizontal annular flow boiling of pure and mixed refrigerants*, Int.J. Heat and Mass Transfer, Vol. 32, N.12, pp. 2435-2446, 1989
14. Soliman, M., *A general correlation for annular flow condensation*, Trans. ASME, J. Heat Transfer, 90 , pp. 267-276, 1968
15. Perry and Chilton editors, *Chemical Engineering Handbook*, 5th Ed., McGraw Hill, 1975
16. Shah, R.K., and London, A., L., *Laminar Flow Forced Convection in Ducts*, Academic Press, New York, 1978
17. Gnielinski, V., *New equations for heat and mass transfer in turbulent pipe and channel flow*, International Chemical Engineering, Vol. 16, No 2, pp 359-368, April 1976

18. Petukhov, B.S., Kurganov, V.A. and Gladuntsov, A.I., *Heat transfer in turbulent pipe flow of gases with variables properties*, Heat Transfer - Soviet Research, Vol. 5, No. 4, pp 109-116, July-August 1973

19. Nitheanandan, T., Soliman, H.M. and Chant, R.E., *A proposed approach for correlating heat transfer during condensation inside tubes*, ASHRAE Transactions 1990, Volume 96, Part 1, page 230-241.

20. Akers, W.W. and Rosson, H.F., *Condensation inside a horizontal tube*, Chemical Engineering Symposium Series, Vol. 56, N° 30, pp. 145-149, 1960

21. Soliman, H.M., T*he mist-annular transition during condensation and its influence on the heat transfer mechanism*, Int. J. Multiphase Flow, Vol. 12., No. 2, pp. 277-288, 1986

22. Shah, M.M., *A general heat transfer correlation for heat transfer during film condensation inside pipes*, International Journal of Heat and Mass Transfer, Vol. 22, pp. 547-556, 1979

23. Jung, D.S. et al., A study of flow boiling heat transfer experiments with refrigerant mixtures, Int.J. Heat and Mass Transfer, Vol. 32, N.9, pp. 1751-1764, 1989

24. Jung, D., Radermacher, R., *Prediction of evaporation heat transfer coefficient and pressure drop of refrigerant mixtures*, International Journal of Refrigeration, Volume 16, No.5, 1993

25. Bensafi, A., *Wide boiling refrigerant mixtures for power savings*, PhD Thesis, The University of Leeds, U.K., 1994

26. Cavallini, A. et. al, *Condensation of new refrigerants inside smooth and enhanced tubes*, Proc. Int. Congress of Refrigeration, The Hague, Netherlands, Tome IVa, pp. 105-114, 21-25 August 1995

27. Rich, D.G. , *Efficiency and thermal resistance of circular fins and rectangular fins*, Proceedings of the Third International Heat Transfer Conference (Vol. III), AIChE-ASME, August 1986

28. Bensafi, A., *Propriétés thermodynamiques et thermophysiques des mélanges de fluides frigorigènes à base de R32/R125/R134a*, CETIAT, Note Technique N° 95 019, Mars 1995

29. Gayet, Ph., Bontemps, A., Marvillet, Ch., *Condensation of mixed vapours of R22 and R114 refrigerants inside horizontal tubes*, Proc. 1st European Conference on Thermal Sciences, Birmingham, U.K., in IChemE Syposium Series No 129, Sept. 1982

30. Bell, K., J., Ghaly, M.A., *An approximate generalized design method for multicomponent/partial condenser*, AICHE Symp. Series, Vol. 69., pp. 72-79, 1976

31. Bivens, D.B., and Yokozeki, A., *Heat transfer coefficients and transport properties for alternative refrigerants*, Proc. International Refrigeration Conference at Purdue, Purdue University, West Lafayette, Indiana, USA, July 1994

32. Ebisu, T. and Torikoshi, K., *Experimental studies on crossflow heat exchanger performance using non-azeotropic refrigerant mixtures*, Proc. Int. Congress of Refrigeration, The Hague, Netherlands, 21-25 August 1995, Tome IVa, pp. 163-170

NOMENCLATURE

A	area
a	constant for 'j' factor
	parameter in refrigerant heat transfer correlation
Bo	Bond number
Cp	heat capacity
D	tube diameter
dt	temperature difference
e	thickness
f	friction factor
F	heat transfer enhancement factor
Fc	correction factor for cross-flow
Fr	Froude number
g	gravity acceleration
G	mass flux
H	enthalpy
h	local heat transfer coefficient
j	factor for air HTC calculation
$(L/D)_{eq}$	equivalent length of tubing
k, K	thermal conductivity
K_{res}	lumped fin resistances factor
L	tube length
M	mass flow rate
n	constant for 'j' factor
	number of grooves per tube
	parameter in refrigerant heat transfer correlation
Nu	Nusselt number
P	pressure
Pr	Prandtl number
Q	heat transferred
Re	Reynolds number
R_{eff}	fin efficiency resistance factor
t	fin thickness
T	temperature
U	overall heat transfer coefficient
x	vapour quality
X_{cr}	dry-out quality
X_{tt}	Lockhart-Martinelli pressure drop parameter

Greek

β	fin angle
Δ	change in quantity
ε	void fraction
ΔT_{LM}	log mean temperature difference
μ	dynamic viscosity
ρ	density
γ	groove helix angle
υ	kinematic viscosity
η	surface effectiveness, fin efficiency

σ	surface tension
Φ	two phase multiplier

Subscripts

a	air
acc	acceleration
avg	average
bt	bare (outside) tube
calc	calculated
exp	experimental
fin	fin
fri	friction
i	element i, inside
in	inlet
int	internal
sat	saturated, at saturation
bend	refers to 180° return bend
L,l, liq	liquid
lo	liquid only
m	mixture
out	outlet
r	refrigerant
res	resistances
t	tube
o	outside
tp	two-phase
tt	turbulent-turbulent
v, vap	vapour
vo	vapour only
w	wall